Chapter 6
An Augmentation Scheme for Fault Tolerant Control Using Integral Sliding Modes

In this chapter a quite different approach is adopted: here an integral sliding mode approach will be retro-fitted to an existing feedback controller. The fault tolerant control allocation scheme in this chapter adopts an a posteri approach, building on an existing state feedback controller designed using only the primary actuators. An integral sliding mode scheme is integrated within the existing controller to introduce fault tolerance. The FTC technique described in this chapter is quite different to the techniques described in Chaps. 3 and 4, which were designed based on the open-loop plant with no cognizance of any existing controller. All the parameters associated with the integral sliding mode schemes in Chaps. 3 and 4 were synthesised simultaneously based on a model of the open-loop plant and specifications for closed-loop performance. In this chapter, for controller design purposes, the actuators are classified as primary and secondary. It is assumed a controller based only on primary actuators has already been designed to provide appropriate closed-loop performance in a fault-free scenario. The idea here is to create an a posteri integral sliding mode design, building on the existing state feedback controller. The idea is to use only the primary actuators in the nominal fault-free scenario, and to engage the secondary actuators only if faults or failures occur. Crucially, in the fault-free case, the closed-loop system behaviour is entirely dependent on the original controller, and the overall scheme behaves exactly as though the ISM scheme is not present. Only in the fault/failure case does the FTC scheme become active. In this way the integral sliding mode FTC scheme described in this chapter can be retro-fitted to almost any existing control scheme to induce fault tolerance. This requires a totally different design philosophy compared to the schemes discussed in Chaps. 3 and 4. The scheme discussed here has an advantage from an industrial perspective, since it can be retro-fitted to an existing control scheme to induce fault tolerance without the need to remove or alter existing control loops. The scheme in this chapter uses measured or estimated actuator effectiveness levels in order to distribute the control signals among the actuators. The effectiveness of the scheme is tested in simulation using the high fidelity nonlinear RECOVER model.

M.T. Hamayun et al., *Fault Tolerant Control Schemes Using Integral Sliding Modes*, Studies in Systems, Decision and Control 61,
DOI 10.1007/978-3-319-32238-4_6

6.1 System Description and Problem Formulation

An LTI system subject to actuator faults or failures can be modelled (as in the previous chapters) as

$$\dot{x}_p(t) = A_p x_p(t) + B_p W(t) u(t) \tag{6.1}$$

where $A_p \in \mathbb{R}^{n\times n}$, $B_p \in \mathbb{R}^{n\times m}$ and $W(t) \in \mathbb{R}^{m\times m}$ is a diagonal semi-positive definite weighting matrix representing the effectiveness of each actuator where the elements $0 \le w_i(t) \le 1$ for $i = 1, \ldots, m$. If $w_i(t) = 1$, the corresponding ith actuator has no fault, whereas if $1 > w_i(t) > 0$, an actuator fault is present. In a situation where $w_i(t) = 0$, the actuator has completely failed. Suppose the input distribution matrix can be partitioned as

$$B_p = \begin{bmatrix} B_1 & B_2 \end{bmatrix} \tag{6.2}$$

where $B_1 \in \mathbb{R}^{n\times l}$ and $B_2 \in \mathbb{R}^{n\times(m-l)}$ and $l < m$ and $l < n$. Here B_1 is the input distribution matrix associated with the primary actuators and is assumed to be of rank equal to l, whilst B_2 is associated with the secondary actuators which provide redundancy in the system.

Assumption 6.1 It is assumed that the pair (A_p, B_1) is controllable.

For the primary and secondary actuators, the weighting matrix $W(t)$ is also partitioned as

$$W(t) = \mathrm{diag}(W_1(t), W_2(t)) \tag{6.3}$$

where $W_1(t) = \mathrm{diag}(w_1(t), \ldots, w_l(t))$ and $W_2(t) = \mathrm{diag}(w_{l+1}(t), \ldots, w_m(t))$ are the weighting matrices for the primary and secondary actuators respectively. In this chapter, it is assumed that the matrix $W(t)$ is estimated by some FDI scheme, as given in Sect. 3.3.1 or by using a measurement of the actual actuator deflection compared to the demand. In this chapter, again, the estimated value $\widehat{W}(t)$ will not be a perfect estimate of the real effectiveness matrix $W(t)$.

Assumption 6.2 Assume the estimated matrix

$$\widehat{W}(t) = \mathrm{diag}(\widehat{W}_1(t), \widehat{W}_2(t)) \tag{6.4}$$

satisfies the relationship

$$W(t) = (I - \triangle(t))\widehat{W}(t) \tag{6.5}$$

where $\triangle(t) = \mathrm{diag}(\triangle_1(t), \triangle_2(t))$.

Both the uncertainty blocks $\triangle_1(t)$ and $\triangle_2(t)$ are assumed to be diagonal such that $\triangle_1(t) = \text{diag}(\delta_1(t), \ldots, \delta_l(t))$ and $\triangle_2(t) = \text{diag}(\delta_{l+1}(t), \ldots, \delta_m(t))$, where the diagonal elements $\delta_i(t) \in \mathbb{R}$ satisfy $|\delta_i(t)| < \triangle_{max}$ for some $\triangle_{max} > 0$ where

$$\triangle_{max} = \max(\|\triangle_1(t)\|, \|\triangle_2(t)\|) \tag{6.6}$$

The matrices $\triangle_1(t)$ and $\triangle_2(t)$ model the level of imperfection in the fault estimate, and satisfy

$$\begin{aligned} W_1(t) &= (I_l - \triangle_1(t))\widehat{W}_1(t) \\ W_2(t) &= (I_{m-l} - \triangle_2(t))\widehat{W}_2(t) \end{aligned}$$

Since B_1 is assumed to have full column rank equal to l, there exists an orthogonal matrix $T_p \in \mathbb{R}^{n \times n}$ such that

$$T_p B_1 = \begin{bmatrix} 0 \\ B_{21} \end{bmatrix} \tag{6.7}$$

where $B_{21} \in \mathbb{R}^{l \times l}$ (and B_{21} is nonsingular). By a suitable change of coordinates $x \mapsto T_p x_p$ it can be ensured that the input plant distribution matrix has the form

$$T_p B_p = \begin{bmatrix} 0 & B_{12} \\ B_{21} & B_{22} \end{bmatrix} \tag{6.8}$$

where $B_{22} \in \mathbb{R}^{l \times (m-l)}$. Next scale the last l states to ensure $B_{21}^T B_{21} = B_{21} B_{21}^T = I_l$ (i.e. B_{21} is orthogonal). Consequently it can be assumed without loss of generality that the system in (6.1) can be written as

$$\dot{x}(t) = Ax(t) + BW(t)u(t) \tag{6.9}$$

where

$$B = \left[\begin{array}{c|c} 0 & B_{12} \\ B_{21} & B_{22} \end{array}\right] := \left[\, B_o \,\middle|\, B_s \,\right] \tag{6.10}$$

Controllability of (A_p, B_1) implies that the pair (A, B_o) is controllable. Assume that a state feedback control law

$$\nu_o(t) = Fx(t) \tag{6.11}$$

has been designed a priori to make the system

$$\dot{x}(t) = (A + B_o F)x(t) \tag{6.12}$$

stable. Note that the gain F is the baseline controller specifically designed based on the primary actuators. Now a control allocation scheme will be *retro-fitted* to the control law $\nu_o(t)$. The physical control law $u(t)$ applied to *all the actuators* is defined as

$$u(t) = N(t)\nu(t) \tag{6.13}$$

where $\nu(t) \in \mathbb{R}^l$ is the virtual control effort produced by the actuators, and will be discussed in the next section. The overall control structure is given in Fig. 6.1, where it is clear that the integral sliding mode FTC scheme is retro-fitted to the existing baseline controller $\nu_o(t)$ (which is designed based on the primary actuators) and will be only active in the case of faults or failures. The control allocation matrix is given by

$$N(t) = \begin{bmatrix} I_l \\ N_2(t)(I_l - \widehat{W}_1(t)) \end{bmatrix} \tag{6.14}$$

where

$$N_2(t) := B_{22}^T B_{21}(B_{21}^T B_{22}\widehat{W}_2(t)B_{22}^T B_{21})^{-1} \tag{6.15}$$

and $\widehat{W}_1(t)$ and $\widehat{W}_2(t)$ are the estimates of the effectiveness levels. Now define

$$\mathscr{W} = \{(\hat{w}_{l+1}, \ldots, \hat{w}_m) \in \underbrace{[0\ 1] \times \cdots \times [0\ 1]}_{m-l \text{ times}} : \det(B_{22}\widehat{W}_2(t)B_{22}^T) \neq 0\} \tag{6.16}$$

Assumption 6.3 Throughout this chapter, it is assumed that $m \geq 2l$.

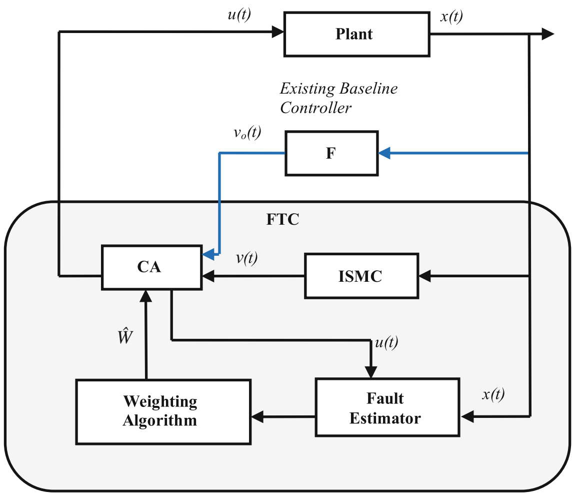

Fig. 6.1 Schematic of the overall control strategy

Remark 6.1 This allows up to $m-2l$ of the entries $\hat{w}_i(t)$ in the matrix $\widehat{W}_2(t)$ to be zero, and yet guarantee $\det(B_{22}\widehat{W}_2(t)B_{22}^T) \neq 0$. The set $\mathscr{W}$ will be shown to constitute the class of faults/failures for which closed-loop stability can be maintained.

Substituting (6.5) and (6.13) into (6.9) yields

$$\dot{x}(t) = Ax(t) + \begin{bmatrix} B_{12}(I_{m-l} - \triangle_2)\widehat{W}_2(t)N_2(t)(I_l - \widehat{W}_1(t)) \\ B_{21}(I_l - \triangle_1)\widehat{W}_1(t) + B_{22}(I_{m-l} - \triangle_2)\widehat{W}_2(t)N_2(t)(I_l - \widehat{W}_1(t)) \end{bmatrix} \nu(t) \tag{6.17}$$

Since B_{21} is orthogonal by construction $B_{21}B_{21}^T = I_l$, then using the definition of $N_2(t)$ in (6.15) it follows that

$$B_{22}\widehat{W}_2(t)N_2(t) = B_{21}B_{21}^T B_{22}\widehat{W}_2(t)N_2(t) \;=\; B_{21} \tag{6.18}$$

Consequently using (6.18), Eq. (6.17) simplifies to

$$\dot{x}(t) = Ax(t) + \begin{bmatrix} B_{12}(I_{m-l} - \triangle_2)\widehat{W}_2 N_2(t)(I_l - \widehat{W}_1) \\ B_{21}(I_l - \triangle_1)\widehat{W}_1 + B_{21}(I_l - \widehat{W}_1) - B_{22}\triangle_2\widehat{W}_2 N_2(t)(I_l - \widehat{W}_1) \end{bmatrix} \nu(t) \tag{6.19}$$

which can be further simplified to

$$\dot{x}(t) = Ax(t) + \underbrace{\begin{bmatrix} B_{12}(I_{m-l} - \triangle_2)\widehat{W}_2(t)N_2(t)(I_l - \widehat{W}_1(t)) \\ B_{21} - B_{21}\triangle_1\widehat{W}_1(t) - B_{22}\triangle_2\widehat{W}_2(t)N_2(t)(I_l - \widehat{W}_1(t)) \end{bmatrix}}_{\widehat{B}(t)} \nu(t) \tag{6.20}$$

Remark 6.2 In the case of perfect estimation of $\widehat{W}(t)$ (i.e. $\triangle(t) = 0$) and when there is no fault in the primary and secondary actuators (i.e. $W_1(t) = I_l$ and $W_2(t) = I_{m-l}$), the system in (6.20) becomes

$$\dot{x}(t) = Ax(t) + B_o\nu(t) \tag{6.21}$$

and so only the primary control channels will be used.

In a fault/failure scenario, to maintain the closed-loop performance near to nominal, the concept of integral sliding mode control is combined with the control law from (6.13) and (6.14). The nominal fault-free system in (6.21) will be used for the design of the augmentation scheme which will be demonstrated in the sequel.

6.2 Integral Sliding Mode Controller Design

First choose the sliding surface as $\mathscr{S} = \{x \in \mathbb{R}^n : \quad \sigma(t) = 0\}$ where the switching function $\sigma(t)$, based on the nominal system (6.12), is defined as

$$\sigma(t) := Gx(t) - Gx(0) - G\int_0^t (A + B_oF)\, x(\tau)d\tau \tag{6.22}$$

where $G \in \mathbb{R}^{l\times n}$ is the design freedom to be selected. The elimination of the reaching phase, ensures the occurrence of the sliding motion throughout the entire response of the system. In this chapter, the design freedom G is selected as

$$G := B_o^T \tag{6.23}$$

where B_o is defined in (6.10). With this choice of G it follows

$$GB_o = B_{21}^T B_{21} = I_l$$

and so this choice of G serves as a pseudo-inverse of the matrix B_o. Also from (6.20)

$$G\widehat{B}(t) = B_{21}^T \left(B_{21} - B_{21}\triangle_1(t)\widehat{W}_1(t) - B_{22}\triangle_2(t)\widehat{W}_2(t)N_2(t)(I_l - \widehat{W}_1(t))\right) \tag{6.24}$$

which will be used when obtaining an expression for the equivalent control. Taking the time derivative of $\sigma(t)$ defined in (6.22) along the system trajectories yields

$$\dot{\sigma}(t) = G\dot{x}(t) - GAx(t) - GB_oFx(t) \tag{6.25}$$

Substituting (6.20) into (6.25), the expression above simplifies to

$$\dot{\sigma}(t) = G\widehat{B}(t)\nu(t) - GB_oFx(t) \tag{6.26}$$

Equating $\dot{\sigma}(t) = 0$, and using the fact that $GB_o = I_l$, the expression for the equivalent control is

$$\nu_{eq}(t) = (G\widehat{B}(t))^{-1}Fx(t) \tag{6.27}$$

The equations of motion governing sliding can be obtained by substituting (6.27) into (6.20) which yields

$$\dot{x}(t) = Ax(t) + \widehat{B}(t)(G\widehat{B}(t))^{-1}Fx(t) \tag{6.28}$$

Adding and subtracting the term $B_oFx(t)$, Eq. (6.28) can be written as

$$\dot{x}(t) = (A + B_oF)x(t) + (\widehat{B}(t)(G\widehat{B}(t))^{-1} - B_o)Fx(t) \tag{6.29}$$

which can be further simplified to

$$\dot{x}(t) = (A + B_oF)x(t) + \begin{bmatrix} B_{12}(I - \triangle_2(t))\widehat{W}_2(t)N_2(t)(I - \widehat{W}_1(t))(G\widehat{B}(t))^{-1} \\ 0_l \end{bmatrix} Fx(t) \tag{6.30}$$

Remark 6.3 Note that in the nominal fault-free case when $W(t) = I$, and in the case of perfect estimation of $\widehat{W}(t)$ matrix, the top row in the second term is zero, and the closed-loop sliding motion is stable. In the case of faults or failures when $\widehat{W}(t) \neq I$, then the second term is not zero and will be treated as unmatched uncertainty.

For the stability analysis which follows, write (6.30) as

$$\dot{x}(t) = (A + B_o F)x(t) + \tilde{B}\tilde{\Phi}(t)Fx(t) \tag{6.31}$$

where

$$\tilde{B} := \begin{bmatrix} B_{12} \\ 0 \end{bmatrix} \tag{6.32}$$

and the time varying uncertain term

$$\tilde{\Phi}(t) := (I_{m-l} - \triangle_2(t))\Psi(t)\left(I_l - \triangle_1(t)\widehat{W}_1(t) - B_{21}^T B_{22}\triangle_2(t)\Psi(t)\right)^{-1} \tag{6.33}$$

where

$$\Psi(t) := \widehat{W}_2(t)N_2(t)(I_l - \widehat{W}_1(t)) \tag{6.34}$$

From (6.18) it is clear that $\widehat{W}_2(t)N_2(t)$ is a right pseudo-inverse for $B_{21}^T B_{22}$. Then by using arguments similar to those given in Chap. 3, it follows $\|\widehat{W}_2(t)N_2(t)\| < \gamma_1$ for some positive scalar γ_1, provided that $\det(B_{22}\widehat{W}_2(t)B_{22}^T) \neq 0$. Since

$$\|\Psi(t)\| \leq \|(I_l - \widehat{W}_1(t))\|\|\widehat{W}_2(t)N_2(t)\| < \|\widehat{W}_2(t)N_2(t)\| < \gamma_1$$

the term $\|\Psi(t)\|$ is bounded. Define γ_1^* as the smallest number (which will be used later in Proposition 6.1) satisfying

$$\|\Psi(t)\| < \gamma_1^* \tag{6.35}$$

In the following subsections the main results of the chapter are presented.

6.2.1 Stability Analysis of the Closed-Loop Sliding Motion

In the case of perfect estimation of the $\widehat{W}(t)$ matrix, (i.e. $\triangle(t) = 0$) and when there are no faults in the system (i.e. $W(t) = I$) the uncertain term $\tilde{\Phi}(t)$ in (6.31) vanishes (i.e. $\tilde{\Phi}(t) = 0$) and the closed-loop sliding motion in (6.31) simplifies to

$$\dot{x}(t) = (A + B_o F)x(t) \tag{6.36}$$

which is stable by choice of the baseline controller F.

In the case of non-perfect estimation of $\widehat{W}(t)$, and in the presence of faults, the stability of (6.31) needs to be proven. To this end, in this most general situation the equation governing the sliding motion in (6.31) can be written as

$$\dot{x}(t) = \underbrace{(A + B_o F)}_{\tilde{A}} x(t) + \tilde{B} \overbrace{\tilde{\Phi}(t) \underbrace{Fx(t)}_{\tilde{y}(t)}}^{\tilde{u}(t)} \tag{6.37}$$

For the subsequent stability analysis, define the $\mathscr{L}_2$ gain between $\tilde{u}$ to $\tilde{y}$ as

$$\gamma_2 = \|\tilde{G}(s)\|_\infty \tag{6.38}$$

where the transfer function matrix

$$\tilde{G}(s) := F(sI - \tilde{A})^{-1}\tilde{B} \tag{6.39}$$

which is stable by design.

Proposition 6.1 *Suppose that the condition*

$$(1 + \gamma_3\gamma_1^*)\triangle_{max} < 1 \tag{6.40}$$

holds, where γ_1^* and $\triangle_{max}$ are defined in (6.35) and (6.6) and $\gamma_3 = \|B_{22}\|$, then during fault/failure conditions, including the failure of primary actuators, and for any $\hat{w}_{l+1}(t), \ldots, \hat{w}_m(t) \in \mathscr{W}$ where $\mathscr{W}$ is defined in (6.16), the closed-loop system in (6.37) will be stable if:

$$\frac{\gamma_2\gamma_1^*(1 + \triangle_{max})}{1 - (1 + \gamma_3\gamma_1^*)\triangle_{max}} < 1 \tag{6.41}$$

where γ_2 is defined in (6.38).

Proof The closed-loop sliding motion in (6.37) can be written as

$$\dot{x}(t) = \tilde{A}x(t) + \tilde{B}\tilde{u}(t) \tag{6.42}$$

$$\tilde{y}(t) = Fx(t) \tag{6.43}$$

where

$$\tilde{u}(t) = \tilde{\Phi}(t)\tilde{y}(t) \tag{6.44}$$

By using the small gain theorem (as discussed in Appendix B.1.2), the feedback interconnection of the known stable matrix $\tilde{G}(s)$ with the bounded uncertain term $\tilde{\Phi}(t)$, and hence Eq. (6.37), will be stable if

$$\|\tilde{G}(s)\|_\infty \|\tilde{\Phi}(t)\| < 1 \tag{6.45}$$

From Eq. (6.33), it is clear that

$$\|\tilde{\Phi}(t)\| \leq \|\big(I_l - \underbrace{\triangle_1(t)\widehat{W}_1(t) - B_{21}^T B_{22}\triangle_2(t)\Psi(t)}_{X(t)}\big)^{-1}\|\|(I_{m-l} - \triangle_2(t))\Psi(t)\| \tag{6.46}$$

Using the fact that $\|\widehat{W}_1(t)\| \leq 1$, and $\|B_{21}^T\| = 1$ (since $B_{21}^T B_{21} = I_l$), from (6.46)

$$\begin{aligned}\|X(t)\| &\leq \|\triangle_1(t)\widehat{W}_1(t)\| + \|B_{21}^T B_{22}\triangle_2(t)\Psi(t)\| \\ &\leq \|\triangle_1(t)\| + \|B_{22}\|\|\triangle_2(t)\|\|\Psi(t)\| \\ &\leq (1 + \gamma_3\gamma_1^*)\triangle_{max} < 1\end{aligned}$$

if the conditions of Proposition 6.1 hold. Hence from (6.46), and using the fact that in general

$$\|(I - X)^{-1}\| \leq (1 - \|X\|)^{-1} \quad \text{if} \quad \|X\| < 1$$

it follows that

$$\|\tilde{\Phi}(t)\| \leq \frac{\gamma_1^*(1 + \triangle_{max})}{1 - (1 + \gamma_3\gamma_1^*)\triangle_{max}} \tag{6.47}$$

From the expression in (6.47) and the fact that $\|\tilde{G}(s)\|_\infty = \gamma_2$, a sufficient condition to ensure the small gain theorem in (6.45) holds, is that

$$\frac{\gamma_2\gamma_1^*(1 + \triangle_{max})}{1 - (1 + \gamma_3\gamma_1^*)\triangle_{max}} < 1$$

This is the condition in (6.41), and the proof of Proposition 6.1 is complete. ■

Remark 6.4 If B_{12} is zero in (6.32) which is the assumption in many CA schemes,[1] then $\widetilde{B} = 0$, and the condition of Proposition 6.1 is trivially satisfied. The scheme in this chapter allows $B_{12} \neq 0$, and consequently considers a more general solution, which helps target a wider range of potential applications.

6.2.2 Integral Sliding Mode Control Laws

Now a control law will be designed such that the sliding motion on the sliding surface in (6.22) can be ensured. Define the integral sliding mode control law as

$$\nu(t) = \nu_l(t) + \nu_n(t) \tag{6.48}$$

[1] See for example [1, 2].

where the linear part of the control law (which is known a priori) is

$$\nu_l(t) := Fx(t) \tag{6.49}$$

and the nonlinear part, which induces the sliding motion, is

$$\nu_n(t) := -\rho(t,x)\frac{\sigma(t)}{\|\sigma(t)\|} \qquad \text{for } \sigma(t) \neq 0 \tag{6.50}$$

where $\rho(t,x)$ is the modulation gain whose precise value is given in the statement of Proposition 6.2. Now in the sequel it is demonstrated that the integral sliding mode control law in (6.48)–(6.50) satisfies the reachability condition.

Proposition 6.2 *Assume the conditions of Proposition 6.1 hold. Then if $\rho(t,x)$ is chosen as*

$$\rho(t,x) \geq \frac{(1+\gamma_3\gamma_1^*)\triangle_{max}\|\nu_l(t)\| + \eta}{1-(1+\gamma_3\gamma_1^*)\triangle_{max}} \tag{6.51}$$

where $\eta > 0$ is a small positive scalar, the integral sliding mode control law in (6.48)–(6.50) satisfies the reachability condition and sliding on $\mathscr{S}$ in (6.22) is maintained.

Proof By substituting the control law in (6.48)–(6.50) into (6.26) and by using the fact that $GB_o = I$:

$$\dot{\sigma}(t) = (G\widehat{B}(t))\,(\nu_l(t) + \nu_n(t)) - Fx(t) \tag{6.52}$$

Since by construction $B_{21}^T B_{21} = I_l$, using (6.24) and (6.34), Eq. (6.52) can be written as

$$\begin{aligned}\dot{\sigma}(t) &= (I_l - \triangle_1(t)\widehat{W}_1(t) - B_{21}^T B_{22}\triangle_2(t)\Psi(t))(\nu_l(t) + \nu_n(t)) - Fx(t)\\ &= \nu_n(t) - (\triangle_1(t)\widehat{W}_1(t) + B_{21}^T B_{22}\triangle_2(t)\Psi(t))(\nu_l(t) + \nu_n(t))\end{aligned} \tag{6.53}$$

Now consider the candidate Lyapunov function

$$V(t) = \frac{1}{2}\sigma^T(t)\sigma(t) \tag{6.54}$$

Taking the time derivative of (6.54) and substituting for $\dot{\sigma}(t)$ from (6.53) yields

$$\begin{aligned}\dot{V}(t) &= -\rho(\cdot)\|\sigma\| - \sigma^T(\triangle_1(t)\widehat{W}_1(t) + B_{21}^T B_{22}\triangle_2(t)\Psi(t))(\nu_l(t) + \nu_n(t))\\ &\leq -\rho(\cdot)\|\sigma\| + \|\sigma\|(\triangle_{max} + \gamma_3\triangle_{max}\gamma_1^*)(\|\nu_l\| + \rho(\cdot))\\ &\leq -\rho(\cdot)(1-(\triangle_{max} + \gamma_3\triangle_{max}\gamma_1^*))\|\sigma\| + \|\sigma\|(\triangle_{max} + \gamma_3\triangle_{max}\gamma_1^*)\|\nu_l\|\end{aligned} \tag{6.55}$$

where $\triangle_{max}$ is defined in (6.6). By choosing the value of $\rho(t,x)$ as in (6.51), the expression in (6.55) becomes $\dot{V}(t) \leq -\eta\|\sigma(t)\| = -\eta\sqrt{2V(t)}$, which is the standard reachability condition, and is sufficient to guarantee that sliding on the surface $\mathscr{S}$ is maintained. ■

Finally in order to obtain the overall physical control law which is used to create the actual control signals sent to all the available control surfaces, substituting (6.48)–(6.50) into (6.13) yields

$$u(t) = \begin{bmatrix} I_l \\ N_2(t)(I_l - \widehat{W}_1(t)) \end{bmatrix} \left(Fx(t) - \rho(t,x) \frac{\sigma(t)}{\|\sigma(t)\|} \right) \tag{6.56}$$

where $N_2(t)$ is defined in (6.15). The efficacy of the scheme is tested in the following section using the high fidelity nonlinear model of the large transport aircraft from Appendix A.

6.3 Case Study: Yaw Damping of a Large Transport Aircraft

The integral sliding mode FTC scheme described in this chapter employs an a posteri approach building on an existing state feedback controller designed using only the primary actuators. In the physical control law given in (6.56), the baseline control law F is assumed to exist a-priori. The technique implemented in the FTC scheme is to use the baseline controller in the nominal fault-free scenario, and activate the fault tolerant features only in the case when faults or failures occur in the actuators. All the simulations that follow are based on the RECOVER benchmark model of a large passenger aircraft (see Appendix A.1).

The objective of the simulations is to damp the lateral dynamics of the aircraft when the initial sideslip $\beta(0)$ is perturbed by 1 deg while the aircraft is flying at a high altitude (12,192 m) at a high speed (236 m/s). The lateral dynamics of the aircraft discussed in Appendix A.1 are used to evaluate the scheme. For yaw damping, the washout filter state:

$$\dot{x}_{wo} = r - 0.333x_{wo} \tag{6.57}$$

is augmented with the lateral dynamics, where r is the yaw rate and x_{wo} is the washout filter state. The nominal state feedback controller F associated with the primary actuators for yaw damping (which is a stability augmentation system for the lateral dynamics of an aircraft) has been taken from the literature[2] and is not part of the design process.

By augmenting the washout filter state given in Eq. (6.57), with the aircraft's lateral dynamics the state-space representation of the model is given as

[2]Specifically the control law is based on eigenstructure assignment [3].

$$A_p = \begin{bmatrix} -0.3330 & 0 & 0 & 1 & 0 \\ 0 & 0 & 0 & 0.0816 & 1 \\ 0 & 0.0413 & -0.0537 & -0.9944 & 0.0823 \\ 0 & -0.0012 & 0.6090 & -0.0869 & -0.0335 \\ 0 & 0.0002 & -2.9236 & 0.3681 & -0.4514 \end{bmatrix}$$
$$B_p = \left[\begin{array}{cc|cccc} 0 & 0 & 0 & 0 & 0 & 0 \\ 0 & 0 & 0 & 0 & 0 & 0 \\ 0.0070 & 0 & 0.0003 & -0.0003 & 0.0002 & -0.0002 \\ -0.4438 & -0.0082 & -0.0046 & 0.0046 & 0.0493 & -0.0493 \\ 0.1451 & -0.1329 & -0.0625 & 0.0625 & 0.0085 & -0.0085 \end{array}\right] \tag{6.58}$$

The states are $(x_{wo}, \phi, \beta, r, p)$, where x_{wo} is the washout filter state (rad) in Eq. (6.57), ϕ is the roll angle (rad), β is the side slip (rad), r is the yaw rate (rad/s) and p is the roll rate (rad/s). The control surfaces which are considered for the design are $\delta_{lat} = (\delta_r, \delta_a, \delta_{sp5}, \delta_{sp8}, Tn_l, Tn_r)$ where δ_r is the rudder deflection (rad), δ_a is the aileron deflection (rad), δ_{sp5} is the left inboard spoiler (rad), δ_{sp8} is the right inboard spoiler (rad) and Tn_l and Tn_r are aggregated engine thrusts (N) (scaled by 10^5) on the left and right wing. It is assumed that the left aileron moves in an anti-symmetrical fashion to the right aileron.[3] In (6.58) the input distribution matrix B_p is divided into primary (δ_r, δ_a) and secondary $(\delta_{sp5}, \delta_{sp8}, Tn_l, Tn_r)$ actuators. A further transformation is required in order to have the structure in (6.10) and to ensure that $B_{21}B_{21}^T = I_2$.

6.3.1 Baseline Controller

Eigenstructure assignment is a method that provides the freedom to allow the appropriate set of eigenvalues and associated eigenvectors to be considered in the design procedure to achieve the desired performance or shape of the closed-loop system response. The feedback gain F, based only on the primary actuator, is assumed to be available a priori and should stabilise the nominal closed-loop system in (6.12). The design of F is based on a set of eigenvalues and the best possible eigenvectors. Based on this available eigenstructure, the feedback gain F can be obtained using the relation

$$(A + B_o F)v_i = \lambda_i v_i \quad i = 1, \ldots, n \tag{6.59}$$

where λ_i is an eigenvalue and v_i is the associated eigenvector.

The ideal closed-loop eigenvalues for the nominal state feedback controller F associated with the primary actuators for yaw damping are

$$\{-0.0051, -0.468, -0.6 \pm 0.628j, -1.106\} \tag{6.60}$$

[3] The outboard ailerons and spoilers $(sp1 - 4, sp9 - 12)$ are not active at a high speed cruise condition due to structural limit. The spoilers $(sp6, sp7)$ are ground spoilers and not used in flight.

The motions corresponding to the stable real poles are referred to as the spiral mode (−0.0051), the washout filter (−0.468) and the roll mode (−1.106). The motion corresponding to the complex poles is referred to as the Dutch roll mode. The best possible eigenvectors to ensure decoupling between these modes are

$$\underbrace{\begin{bmatrix} * \\ 0 \\ 1 \\ * \\ * \end{bmatrix} \begin{bmatrix} * \\ 0 \\ 1 \\ * \\ * \end{bmatrix}}_{\text{Dutch roll mode}} \quad \underbrace{\begin{bmatrix} * \\ 1 \\ 0 \\ * \\ * \end{bmatrix}}_{\text{roll mode}} \quad \underbrace{\begin{bmatrix} * \\ 1 \\ 0 \\ * \\ * \end{bmatrix}}_{\text{spiral mode}} \quad \underbrace{\begin{bmatrix} 0 \\ 0 \\ 0 \\ 1 \\ 0 \end{bmatrix}}_{\text{washout filter}} \quad \underbrace{\begin{bmatrix} x_{wo} \\ \phi \\ \beta \\ r \\ p \end{bmatrix}}_{x(t)} \tag{6.61}$$

where $*$ denotes that the value of the element is unimportant. This selection of eigenvectors ensures no coupling of Dutch roll with the roll angle and/roll rate. Furthermore the spiral mode and roll mode are associated with the roll angle only, and should ensure decoupling from the sideslip angle to avoid sideslip in the course of a steady turn. The washout filter which is used for the yaw damping is only associated with the yaw rate. Using the set of eigenvalues and eigenvectors given in (6.60) and (6.61), the ideal baseline control law F for yaw damping (considering only the primary actuators (δ_r, δ_a)), based on eigenstructure assignment is

$$F = \begin{bmatrix} -0.5342 & -0.4817 & 0.0665 & 1.1836 & -0.0133 \\ -21.9319 & -0.5188 & 0.1313 & 1.9001 & 0.6705 \end{bmatrix} \tag{6.62}$$

The state feedback control gain matrix in (6.62) will be taken as the a priori given controller around which the integral sliding mode scheme is created.

6.3.2 *Fault Tolerant Control*

In the case of faults or failures, the baseline control law in (6.62) cannot be used alone; instead the fault tolerant control law given in (6.56) will be employed to retain performance close to the nominal. In the nominal case, the aileron is the primary control surface for ϕ tracking, and the spoilers are the redundancy; whereas the rudder is the primary control surface for β tracking (i.e. yaw damping), and differential engine thrust is the redundancy. The closed-loop stability condition in (6.41) should be guaranteed in nominal and in fault/failure scenarios. The value of γ_2 for the a priori F using Eq. (6.38) is $\gamma_2 = 0.0424$. Using (6.35) it can be verified using a numerical search that $\gamma_1^* = 7.5920$. Hence to satisfy the stability conditions of Proposition 6.1 in (6.40) and (6.41) where $\gamma_3 = 0.7176$, the maximum value of the error in estimation of the actuator effectiveness levels which can be handled by the physical control law in (6.56) is $\triangle_{max} = 10\,\%$.

6.3.3 Nonlinear Simulation Results

As in previous chapters, the discontinuity in the unit vector has been smoothed using the sigmoidal approximation $\frac{\sigma(t)}{\|\sigma(t)\|+\delta}$ given in Sect. 2.5, where the value of the positive scalar is chosen as $\delta = 0.01$. In the sequel three simulation case studies are investigated: one a fault-free case considering the estimation of the $W(t)$ matrix is perfect; the second considering the same scenario as in case 1, but when the estimation of the $W(t)$ matrix is imperfect; and the third a scenario involving a primary actuator failure with imperfect estimation of $W(t)$.

6.3.3.1 Case 1: Fault-Free Case with Perfect Estimation of $W(t)$

In the case when the estimation of the effectiveness level matrix $W(t)$ is perfect, $\triangle(t) = 0$ and $\triangle_{max} = 0$. Consequently the stability condition in (6.41) reduces to $\gamma_2\gamma_1^* = 0.3217 < 1$. Figures 6.2 and 6.3 demonstrate the nominal fault-free performance. In Fig. 6.2 it can be seen that the roll and yaw modes are decoupled. During the nominal fault-free scenario the secondary actuators are not active (Fig. 6.3) because the integral sliding mode FTC scheme is not active in this case, and only the baseline controller F is employed to achieve the nominal performance.

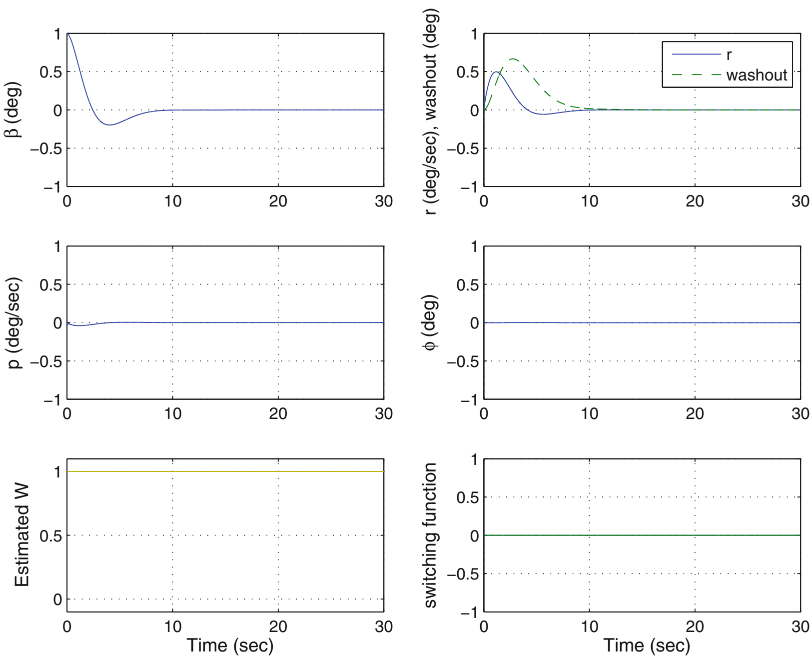

Fig. 6.2 No fault (perfect estimation of $W(t)$): plant states

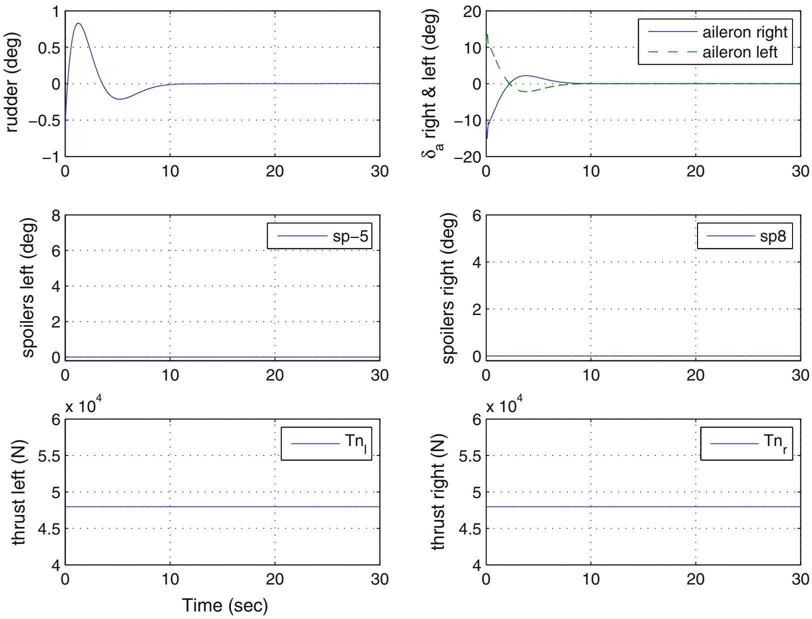

Fig. 6.3 No fault (perfect estimation of $W(t)$): actuators

6.3.3.2 Case 2: Fault-Free Case with Imperfect Estimation of $W(t)$

A second scenario is considered here to demonstrate the efficacy of the scheme when the system is fault-free and the estimation of the $W(t)$ matrix is not perfect. Figure 6.4 shows that due to imprecise information provided by the FDI, the estimate $\widehat{W}(t) \neq I$, (indicating the presence of faults) although in reality there is no fault in the system. In response to this the control allocation scheme engages the secondary actuators (spoilers for ϕ performance and differential engine thrust for β performance) as shown in Fig. 6.5 to maintain closed-loop stability of the system and to retain nominal performance as in Fig. 6.2.

6.3.3.3 Case 3: Primary Failure with Imperfect Estimation of $W(t)$

The third scenario demonstrates the scheme with imperfect estimates $\widehat{W}(t)$ in the case of failures in the primary actuators. Theoretically the maximum percentage error $\triangle_{max}$ the scheme can handle and yet ensure the stability conditions of Proposition 6.1, is 10 %. Figure 6.7, shows the scenario when both the primary actuators (rudder and ailerons) have jammed at offset positions at 6 s, and due to imprecise information provided by the FDI scheme, the effectiveness of the primary actuators is estimated at 10 %, instead of 0 % (Fig. 6.6). Due to this failure, the right wing spoiler $sp8$ is actively engaged by the control allocation scheme, together with the left and right

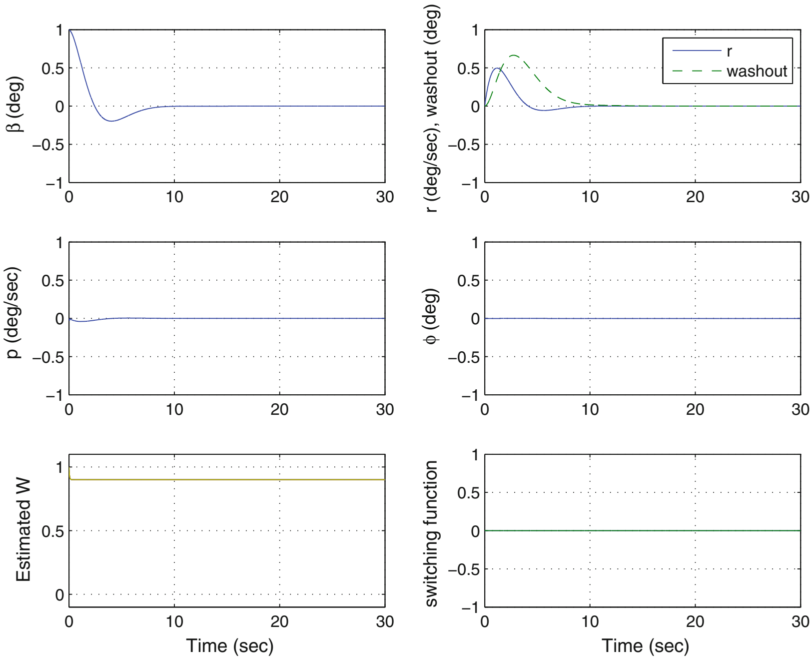

Fig. 6.4 No fault (imperfect estimation of $W(t)$): plant states

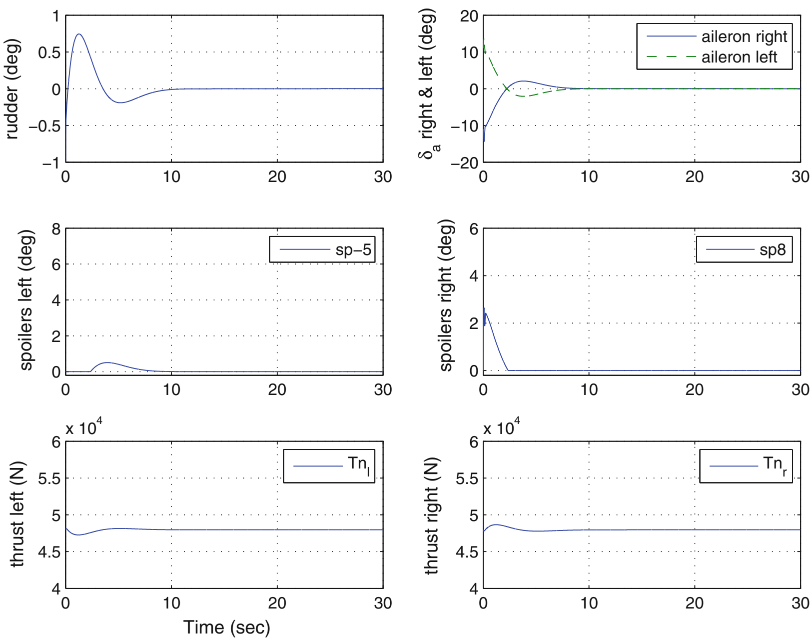

Fig. 6.5 No fault (imperfect estimation of $W(t)$): actuators

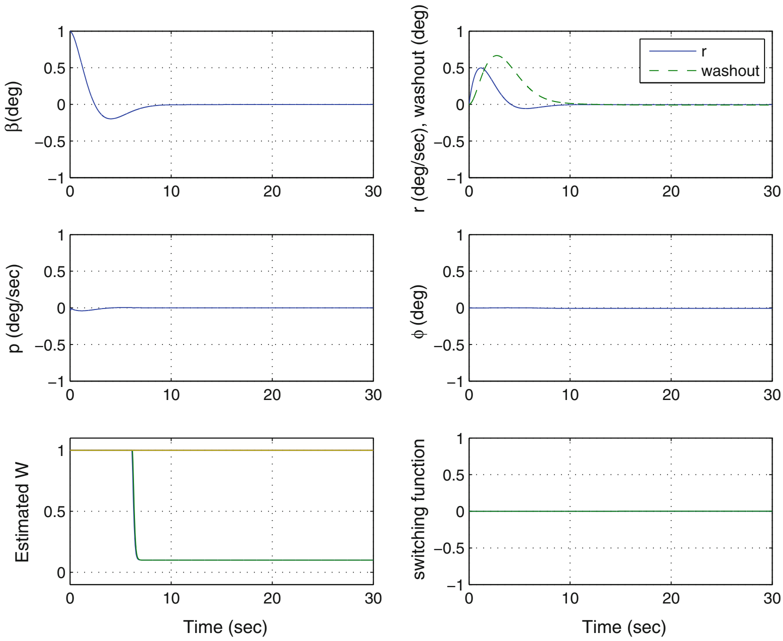

Fig. 6.6 Primary failure (imperfect estimation of $W(t)$): plant states

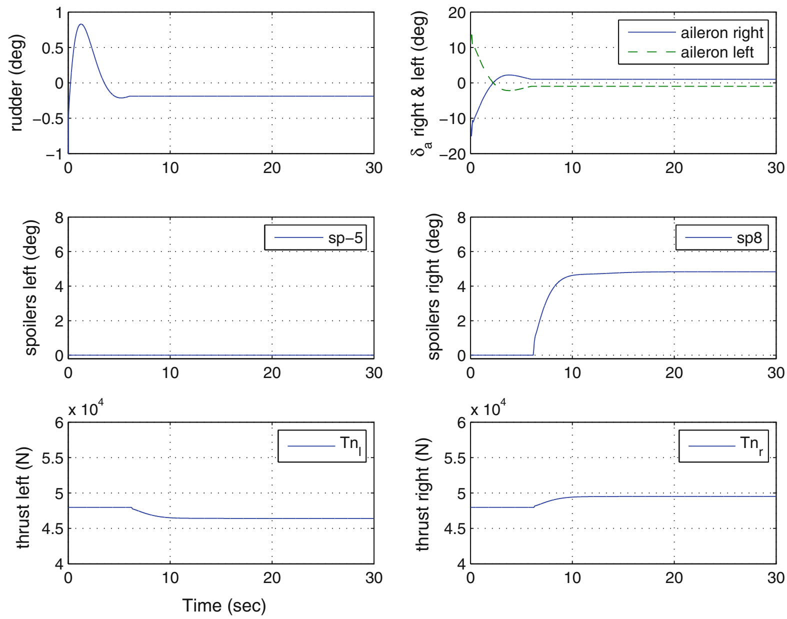

Fig. 6.7 Primary failure (imperfect estimation of $W(t)$): actuators

wing engine thrusts, to cope with this situation, and to maintain performance close to the nominal (Fig. 6.7). The switching function plot in Fig. 6.7 shows that sliding is maintained during the entire system response.

6.4 Summary

This chapter described a fault tolerant control scheme incorporating integral sliding mode and CA, based on an a posteri approach. Here an ISM and CA architecture was incorporated into an existing state feedback controller (designed using only the primary actuators). As in earlier chapters, to distribute the control signals to the functional actuators, the scheme uses the estimated effectiveness levels of the actuators provided by an FDI scheme. The efficacy of the FTC scheme was tested in simulation using the high fidelity nonlinear RECOVER benchmark model.

6.5 Notes and References

Retro-fitting a new component to an existing baseline feedback control scheme to achieve fault tolerance is appealing because it retains the performance of baseline controller nominally. The nominal fault-free performance can be achieved by any design paradigm including $\mathscr{H}_\infty$ control [4], eigenstructure assignment [5], LQR [1], or sliding mode control [6–8]. An early example of retro-fitting adaptive reconfigurable control laws to conventional control laws was explored in [9]. The implementation of retro-fit control laws is possible in a parallel or in an 'in-line' or 'series' approach [10]. In [11], a reconfigurable control effector compensation scheme was proposed, where an adaptive subsystem was implemented in a retro-fit fashion as an add-on signal within the Fast on-Line Actuator Recovery Enhancement (FLARE) system. In [12], a theoretical framework was developed for retro-fitting reconfigurable flight control laws to accommodate severe structural damage and the resulting state dependent disturbances, using prior information about the baseline controller. In [13], a decentralised retro-fitted adaptive FTC scheme was designed for nonlinear models to accommodate loss of effectiveness in flight control actuators. The loss of effectiveness parameters and retro-fit control signals are generated locally to deal with loss of effectiveness in the actuators. In this chapter the baseline yaw damping controller in Sect. 6.3.1 is based on arguments in [14] and the eigenstructure assignment has been performed based on the toolbox associated with [3].

References

1. Härkegård, O., Glad, S.T.: Resolving actuator redundancy—optimal control vs. control allocation. Automatica **41**, 137–144 (2005)
2. Shin, D., Moon, G., Kim, Y.: Design of reconfigurable flight control system using adaptive sliding mode control: actuator fault. Proc. Inst. Mech. Eng. Part G: J. Aerosp. Eng. **219**, 321–328 (2005)
3. Liu, G.P., Patton, R.J.: Eigenstructure Assignment for Control Systems Design. Wiley, Chichester (1998)
4. Ganguli, S., Marcos, A., Balas, G.J.: Reconfigurable LPV control design for Boeing 747-100/200 longitudinal axis. In: Proceedings of the American Control Conference (2002)
5. Duan, G.: Parametric eigenstructure assignment via output feedback based on singular value decompositions. IEE Control Theory Appl. **150**(1), 93–100 (2003)
6. Hess, R.A., Wells, S.R.: Sliding mode control applied to reconfigurable flight control design. J. Guid. Control Dyn. **26**, 452–462 (2003)
7. Shtessel, Y., Buffington, J., Banda, S.: Tailless aircraft flight control using multiple time scale re-configurable sliding modes. IEEE Trans. Control Syst. Technol. **10**, 288–296 (2002)
8. Alwi, H., Edwards, C., Tan, C.P.: Fault Detection and Fault Tolerant Control Using Sliding Modes. Advances in Industrial Control Series. Springer, Berlin (2011)
9. Wohletz, J.M.: Retrofit Systems for Reconfiguration in Civil Aviation. PhD thesis, MIT (2000)
10. Doyle, M.E.: Retrofit reconfigurable flight control system and the F/A-18C. Master's thesis, University of Tennessee - Knoxville (2006)
11. Bošković, J.D., Bergstrom, S.E., Mehra, R.K.: Retrofit reconfigurable flight control in the presence of control effector damage. In: Proceedings of the American Control Conference, pp. 2652–2657 (2005)
12. Bošković, J.D., Prasanth, R., Mehra, R.K.: Retrofit fault-tolerant flight control design under control effector damage. J. Guid. Control Dyn. **30**(3), 703–712 (2007)
13. Bošković, J.D.: A new decentralized retrofit adaptive fault-tolerant flight control design. In: International Journal of Adaptive control and signal Processing (2012)
14. Farineau, J.: Lateral electric flight control laws of a civil aircraft based upon eigenstructure assignment technique. In: American Institute of Aeronautics and Astronautics (1989)